Cell, Vol. 113, 597–607, May 30, 2003, Copyright ©2003 by Cell Press

Development of Genetic Circuitry Exhibiting Toggle Switch or Oscillatory Behavior in *Escherichia coli*

Mariette R. Atkinson,[1] Michael A. Savageau,[2,4] Jesse T. Myers,[2,3] and Alexander J. Ninfa[1,*]
[1]Department of Biological Chemistry
[2]Department of Microbiology and Immunology
[3]Program in Cellular and Molecular Biology
University of Michigan School of Medicine
Ann Arbor, Michigan 48109

Summary

Analysis of the system design principles of signaling systems requires model systems where all components and regulatory interactions are known. Components of the Lac and Ntr systems were used to construct genetic circuits that display toggle switch or oscillatory behavior. Both devices contain an "activator module" consisting of a modified *glnA* promoter with *lac* operators, driving the expression of the activator, NRI. Since NRI activates the *glnA* promoter, this creates an autoactivated circuit repressible by LacI. The oscillator contains a "repressor module" consisting of the NRI-activated *glnK* promoter driving LacI expression. This circuitry produced synchronous damped oscillations in turbidostat cultures, with periods much longer than the cell cycle. For the toggle switch, LacI was provided constitutively; the level of active repressor was controlled by using a *lacY* mutant and varying the concentration of IPTG. This circuitry provided nearly discontinuous expression of activator.

Introduction

The molecular basis by which oscillations in gene expression are sustained in living organisms have long fascinated biologists, and have served as the focal point for intensive investigation using a variety of organisms ranging from cyanobacteria to human. Exciting progress has recently been made in understanding natural circadian clocks. Nevertheless, complex signaling systems, such as natural genetic clocks, represent a difficult challenge for studies of system design principles; one is never certain that the full set of components have been identified, and we often lack detailed knowledge of the biochemical parameters for the known components. Here, we study the minimal gene circuitry required for generating oscillations in gene expression in vivo by constructing a synthetic genetic circuit that produces damped oscillations with a circadian period in *Escherichia coli*. Since the components of such a genetic clock are known at the outset, it may serve as a model system for studies aimed at identifying the principles governing oscillatory behavior.

The first attempts at construction of synthetic genetic circuits for *E. coli* were a toggle switch and an oscillator (Gardner et al., 2000; Elowitz and Leibler, 2000). The toggle switch, consisting of two repressors that control each other's expression, demonstrated bistability and hysteresis (Gardner et al., 2000). The oscillator, consisting of three genes encoding repressors linked in a daisy chain, produced a few noisy oscillations that could be detected in selected single cells by using fluorescence microscopy to score the expression of a GFP reporter (Elowitz and Leibler, 2000).

In a theoretical study, Barkai and Leibler (2000) described a model gene circuit consisting of an activator and a repressor. The activator activated its own expression and that of the repressor; the repressor antagonized the activity of the activator. Analysis showed that, with appropriate parameters, this model produced sustained oscillations and was resistant to noise.

The objective of our project was to develop a genetic clock as a model system for studies of system design principles relevant to natural clocks. At the outset, we established five criteria for the desired clock. (1) It must function in large populations of cells growing in a steady state. (2) Clock behavior must be insensitive to minor alterations in culture conditions. (3) Studies of clock function must require no special equipment, other than a chemostat, and be technically simple. (4) It must be possible to insulate the clock from other signal transduction systems of the cell. (5) The clock must be suitable for regulating any gene, enabling its use in a variety of applications.

Here, we describe the development of a genetic clock and, with altered connectivity, a genetic toggle switch. The promoter region of the *glnALG* operon was modified to include operator sites for the LacI repressor in addition to the normal enhancer sites for activation by NRI∼P. The altered promoter region was then fused to the structural gene for NRI to create an autoregulated circuit. The *glnK* promoter, which also is activated by NRI∼P, was fused to the *lacI* structural gene. The interconnected circuitry resulting from these modifications produced damped oscillations in *E. coli*. When the *lacI* gene is not fused to the *glnK* promoter but expressed constitutively, thereby eliminating the influence of NRI∼P on LacI expression, the alternative connectivity produced toggle-switch behavior.

Results

Model Design and Analysis

We started with a simple circuit incorporating linked activator and repressor modules (Figures 1A and 2A). Our basic model is reminiscent of the theoretical clock of Barkai and Leibler (2000). It consists of an activator module that forms a positive autoregulatory circuit linked to a repressor module. It is unique in that the repressor directly represses transcription of the activator gene, as opposed to antagonizing activator activity. This model was chosen because we anticipated that it would be easier to build and characterize than a clock where repressor antagonizes activator activity.

*Correspondence: aninfa@umich.edu
[4]Present address: Department of Biomedical Engineering, University of California, Davis, One Shields Avenue, Davis, California 95616.

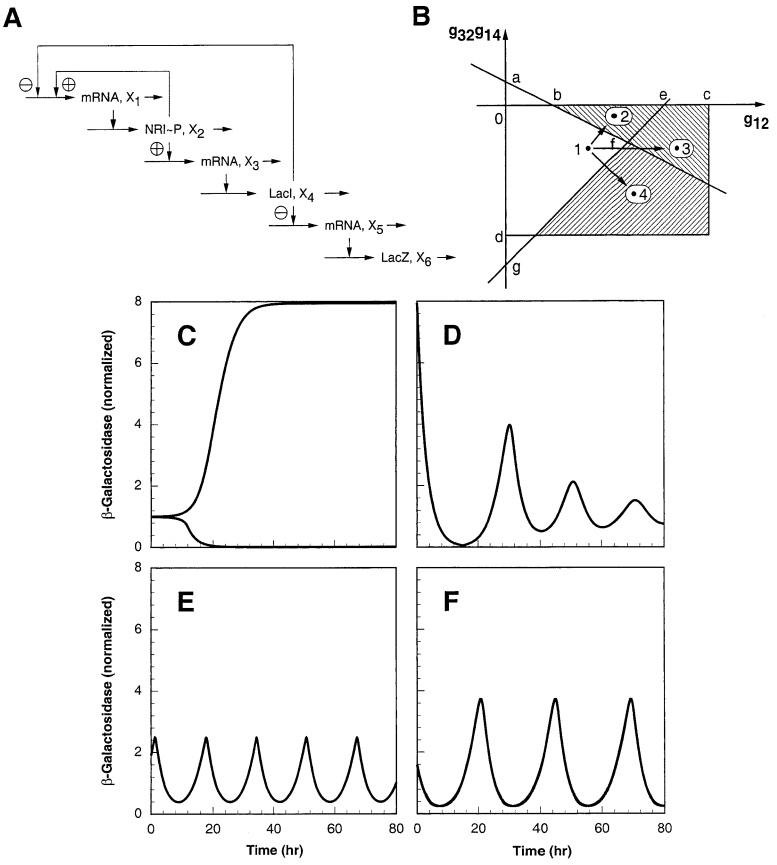

Figure 1. Kinetic Model for a Genetic System Consisting of Linked Positive and Negative Circuits

(A) Clock design. The symbol X_i represents the concentration of a gene product; odd and even subscripts represent mRNA and protein, respectively. Mass fluxes, which characterize the state of the system, correspond to the rate of synthesis and the rate of degradation/dilution of each species and are represented by horizontal arrows; catalytic and regulatory influences are represented by vertical arrows. Activation of transcription is depicted as (+); repression of transcription is depicted as (−). Undepicted factors and precursors are assumed to be constant. NRI is considered equivalent to NRI∼P under the conditions of our experiments. The last 2 horizontal levels of the model represent transcription, translation and removal processes for products of the *lacZYA* operon, which serves as a reporter for the concentration of LacI (X_4).

(B) Design space with a geometry that is completely defined by the kinetic orders and rate constants of the model (not drawn to scale). The key regulatory interactions are represented by kinetic orders that reflect the cooperativity of the interactions. g_{12} and g_{14} are kinetic orders representing the influence of activator NRI∼P (X_2) and repressor LacI (X_4) on the rate of synthesis of NRI mRNA (X_1). g_{32} is the kinetic order representing the influence of activator NRI∼P (X_2) on the rate of synthesis of LacI mRNA (X_3). Each point within this space represents a specific design. The signs of kinetic orders representing effects on transcription ($g_{12} > 0$, $g_{14} > 0$, and $g_{32} > 0$) dictate that only designs in the lower right-hand quadrant of this space are realizable. When perturbed from the steady state, designs represented by points above the line with negative slope are predicted to exhibit dynamic instability that grows exponentially with time (i.e., the solution in the neighborhood of the steady state has a single eigenvalue with positive real part), whereas those below both inclined lines are predicted to exhibit dynamic instability that oscillates with exponentially increasing amplitude (i.e., the solution in the neighborhood of the steady state has 2 complex conjugate eigenvalues with positive real part). Conversely, designs represented by points below the line with negative slope and above that with positive slope are predicted to exhibit locally stable dynamic behavior (i.e., the solution in the neighborhood of the steady state has no eigenvalues with positive real part).

(C) The design represented by a typical point in the top sector (point 2) exhibits switch-like behavior. When initial values of the concentration variables are given by a small perturbation above the steady state, expression is switched fully on; when given by a small perturbation below the steady state, expression is switched fully off. The design represented by a typical point in the right sector (point 3) exhibits essentially the same behavior (data not shown).

(D) The design represented by a typical point in the left sector (point 1) exhibits locally stable behavior with damped oscillations.

(E) The design represented by a typical point in the bottom sector (point 4) exhibits oscillatory instability that grows with time until sustained oscillations are attained (initial transient is not shown).

(F) The design represented by point 1 has been moved into sector 4 by alteration of a parameter that moves the boundary between sectors 1 and 4.

Analysis of the model was conducted by well-established procedures (Supplemental Data available at http://www.cell.com/cgi/content/full/113/5/597/DC1). The results can be conveniently summarized by means of a simple "design space" in which the effects of all parameters are represented (Figure 1B). The axes in this diagram represent regulatory interactions: the kinetic order for activation of the activator module (g_{12}) versus the product of the kinetic orders for activation of the repressor module (g_{32}) and for repression of the activator module (g_{14}). The boundaries defining the "sectors" of this design space are determined by the stability of the mRNA and proteins species. There will always be a line with positive slope and another with negative slope; the slopes of these lines and their intercepts depend upon the half-lives (Supplemental Data available at http://www.cell.com/cgi/content/full/113/5/597/DC1). Any particular design is represented by a point within one of the sectors of this space. The sectors are associated with distinct behaviors; the circuitry could act as a toggle switch (Figure 1C), could generate damped oscillations (Figure 1D), or could generate sustained oscillations (Figure 1E), depending on the values of the parameters.

These results can be used to guide construction of circuitry without detailed knowledge of the biochemical parameters. Once one has constructed an initial circuit, its behavior will suggest its location in design space. Knowing its initial location suggests parameter alterations that will move the design into a region producing the desired behavior. For example, in the construction of a clock, if the initial circuit displays damped oscillatory behavior characteristic of "sector 1" (Figure 1B), it

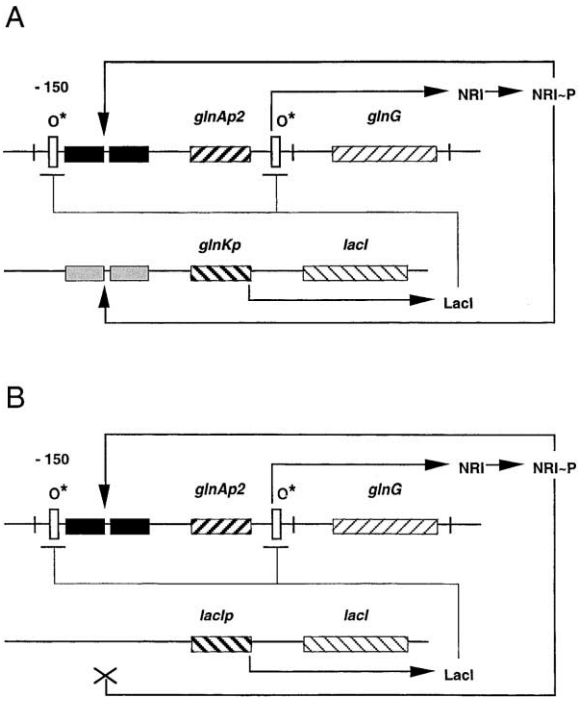

Figure 2. Activator and Repressor Modules of the Genetic Clock and Toggle Switch

(A) Modules and connectivity for the genetic clock. The top construct (activator module) contains the *glnAp2* promoter (heavily hatched box) fused to *glnG* (lightly hatched box). Transcription from *glnAp2* requires the phosphorylated form of the enhancer binding protein NRI (*glnG* product). The high-affinity NRI binding sites are indicated by solid black boxes. This promoter is repressed by LacI binding to 2 perfect *lac* operator sites O* (unfilled boxes). The perfect *lac* operator sites are similar to the natural *lac* O1 sequence, but are palindromes of the left half-site and missing the central base pair of the operator sequence. The bottom construct (repressor module) contains the *glnK* promoter (heavily hatched box) fused to *lacI* (lightly hatched box). The *glnK* promoter also requires NRI∼P for activation, however the enhancer binding sites (solid gray boxes) are less potent than those at *glnAp2*. Activation and repression are depicted by arrowheads and solid bars, respectively.

(B) Modules and connectivity for the toggle switch. The top construct (activator module) is identical to that in (A). The bottom construct (repressor module) is the native LacI transcriptional unit that is expressed constitutively.

should be possible to "move" the clock design into the desired "sector 4," where stable oscillations are observed. This can be accomplished either by adjusting kinetic orders (moving the point from sector 1 to sector 4, e.g., Figure 1E) or by altering rate constants (moving the line that defines the boundary between sector 1 and sector 4 across the point). An example of the latter process is shown in Figure 1F; the design is the same as that producing the results in Figure 1D, except that the lifetime of repressor mRNA ($1/\beta_3$) has been increased 10-fold. Altering this parameter moves the boundary so that the system design now falls within sector 4 and produces stable oscillations.

Construction of the Genetic Clock

We used elements of the *E. coli* Ntr and Lac systems to build the clock (Beckwith, 1987; Ninfa et al., 2000). These parts were chosen because they permit manipulation of the kinetic order of activation and repression of the clock modules, and because the relative position-independence of activator and repressor binding sites simplifies the building of promoters. The activator module consists of a modified *glnA* promoter region fused to the *glnG* (*ntrC*) structural gene for the activator, NRI (NtrC). The *glnAp2* promoter was modified by adding two "perfect" *lacO* operator sequences (*lacO**), one centered at +11 relative to the transcription start site, similar to *lac*, and the other centered at −161 (Figure 2). Our design was intended to permit formation of a repression DNA loop upon engagement of the tetrameric LacI repressor, as occurs at *lac* (Oehler et al., 1990). Since we used two perfect operator sequences, the repression loop formed might be even more stable than the repression loop formed at *lac*.

The σ^{54}-dependent *glnAp2* promoter is activated by the phosphorylated form of NRI, NRI∼P, which binds with high affinity to two adjacent upstream binding sites that constitute the *glnA* enhancer (Ninfa et al., 1987). NRI∼P bound at the enhancer interacts with σ^{54}-RNA polymerase bound at the promoter by means of an activation DNA loop (Su et al., 1990). We envisioned that activator and repressor would act antagonistically because the formation of the activation DNA loop and the repression DNA loop would be mutually exclusive. Also, binding of repressor at the promoter-proximal operator should interfere with the recruitment of polymerase. The *glnA* control region contains a second promoter, *glnAp1*, that overlaps the enhancer and is repressed by NRI∼P (Reitzer and Magasanik, 1985). This promoter, utilized by the main form of RNA polymerase, has the potential to "prime" production of NRI in cells lacking NRI. To complete the activator module, we positioned the structural gene for NRI, *glnG* (*ntrC*), downstream of the modified *glnAp2* promoter. This creates a positive autoregulatory circuit in which NRI activates its own expression. The DNA sequence for this part of the activator module is based upon plasmid pgln53, which causes hyperexpression of NRI (Chen et al., 1982).

NRI activates transcription only when phosphorylated (Ninfa and Magasanik, 1986). In wild-type cells, the kinase/phosphatase NRII (NtrB) brings about phosphorylation of NRI under nitrogen-limiting conditions and dephosphorylation of NRI∼P under nitrogen-excess conditions. To insulate our clock from the cellular nitrogen status, we used a mutant NRII protein, NRII2302 that is partially defective in phosphatase activity and brings about the phosphorylation of NRI under all conditions. While NRII2302 is not completely defective in phosphatase activity, its use under the conditions of our experiments disconnects our clock from the nitrogen status of the cell to a considerable extent. We provided NRII2302 from a multicopy plasmid (not depicted in Figure 2), resulting in slightly higher expression than that of NRII in wild-type cells.

For the repressor module, we used the *glnK* promoter of *E. coli* (Figure 2A), which is dependent on σ^{54}-RNA polymerase and activated by NRI∼P binding to an upstream enhancer (Atkinson et al., 2002b). Unlike the potent *glnA* enhancer, the *glnK* enhancer consists of a high affinity NRI∼P binding site adjacent to a low-affinity NRI∼P binding site. As a consequence, the *glnK* pro-

moter is only activated when the NRI∼P concentration is near its physiological maximum. However, when activated, the promoter is strong (Atkinson et al., 2002b; Blauwkamp and Ninfa, 2002). To complete the repressor module, we replaced the structural gene for *glnK* with the *lacI* gene encoding Lac repressor.

The clock modules were placed on the *E. coli* chromosome in single copy within "landing pads" designed for transcriptional isolation of genes. These landing pads contain restriction sites for cloning located between intrinsic transcription termination sequences. A drug-resistance marker was placed just outside one of the terminators to facilitate transfer of the module by generalized transduction. One of the landing pads, described previously (Simons et al., 1987; Elliot, 1992), was within the *trp* operon. Two others, in the *glnK* and *rbs* regions, were constructed as part of this work (Supplemental Data available at http://www.cell.com/cgi/content/full/113/5/597/DC1). The activator and repressor modules could be placed on either leading or lagging strands of the replicore by cloning into the landing pad in different orientations, followed by recombination onto the chromosome. Repressor and activator modules were assembled in cells containing mutations in the chromosomal *lacI*, *glnG*, and *glnL* genes, such that the only source of LacI was the repressor module, the only source of NRI was the activator module, and the only source of NRII2302 was the plasmid (Supplemental Data available at http://www.cell.com/cgi/content/full/113/5/597/DC1). In these cells, expression of the chromosomal *lacZYA* operon and Ntr genes such as *glnA* (encoding glutamine synthetase) are under the control of the genetic clock.

Experimental Test of the Design

Clock function was synchronized by growing a seed culture in medium containing IPTG, a gratuitous inducer that inactivates Lac repressor. Cells were washed to remove IPTG and used to inoculate a chemostat. Cultures were then incubated in the chemostat in the absence of inducer, with the nutrient flow adjusted to maintain a stable culture density. That is, the chemostat was used as a turbidostat. Effluent from the chemostat was periodically analyzed for reporter gene expression.

Using the combination of modules depicted in Figure 3A, we reproducibly observed damped oscillations with three unambiguous cycles of *lacZYA* expression (Figures 3B and 3D). When grown in defined medium under conditions that resulted in a doubling time of ∼2 hr, the period of the clock was ∼20 hr (Figure 3B). Thus, individual cells inherited information on the state of the clock as they grew and divided. Comparing our synthetic genetic clock to the cyanobacterial clock (Mori et al., 1996), the natural clock routinely provides >10 cycles in similar experiments. (Also, the natural clock is entrainable by light and the period is unaffected by temperature [Kondo et al., 1997]). Nevertheless, our synthetic three-cycle clock with damped oscillations represents a considerable advance over previous synthetic clock circuitry (Elowitz and Leibler, 2000). Clock function could be routinely observed for 70 hr under these conditions without entrainment, indicating considerable resistance to noise. When grown in rich medium under conditions that resulted in a doubling time of ∼1 hr, the period of the clock was ∼11 hr, and three unambiguous cycles were routinely observed in experiments lasting ∼40 hr (Figure 3D). Simulations with model parameters that locate the clock design in sector 1 (Figure 1B) corresponded well to the experimental results (Figures 3C and 3E).

Predicting Optimal Changes in Design

The results in the previous section suggested that our system design was in sector 1 (Figure 1B), and thus we explored the movements in design space that would bring the design into sector 4. The shortest distance, *d*, between the point in sector 1 representing the system design and the boundary to sector 4 is represented by a line from the point perpendicular to the boundary. This distance can be expressed in terms of the geometry of the design space and the parameters in our design. The method for calculating this distance is presented in the Supplemental Data available at http://www.cell.com/cgi/content/full/113/5/597/DC1.

Which parameter, when changed, will most effectively reduce the distance between a point in sector 1 and the boundary to sector 4 to zero? That is, which parameter is the best target to convert a system producing damped oscillations to one producing sustained oscillations? We compared the parameters by varying the value of each about its nominal value and observing the resulting change in the nominal distance to the lower boundary (Figure 4). The effect of altering parameters can be ranked: The cooperativity g_{12} is the most effective, requiring only a ∼10% increase to reduce the distance to zero. Next is the rate constant for degradation of activator β_2, which requires only a slightly larger increase (∼15%). Then is the cooperativity product $g_{14}g_{32}$, but this must increase ∼2.5 fold. Finally, the rate constant for repressor mRNA degradation β_3 would have be decreased ∼5-fold. It is not practical to change the other two parameters. Even a 100-fold increase in the rate constant for activator mRNA degradation β_1 does not reduce the distance to zero. Although decreasing the rate constant for repressor degradation β_4 by ∼15% would reduce the distance to zero, repressor is already a very stable protein and increasing its stability further is impractical. Thus, the best strategy for generating sustained oscillations would be decrease the lifetime of the activator protein, increase the lifetime of the repressor mRNA, and increase the cooperativity of the regulatory interactions.

Sampling Design Space by Manipulating the Relative Copy Numbers of the Activator and Repressor Modules

The activation of the activator module *glnAp2* promoter is expected to display an S-shaped kinetic profile. At low concentrations of activator (X_2), below the threshold for activation, there will be little expression from the promoter and the kinetic order with respect to X_2 is nearly zero. As X_2 is increased into the range of regulating concentrations, the promoter is activated with a kinetic order dependent on features of the construction, such as enhancer strength and the spacing of promoter and enhancer. Finally, at high X_2 concentrations, the promoter is fully activated and the kinetic order with

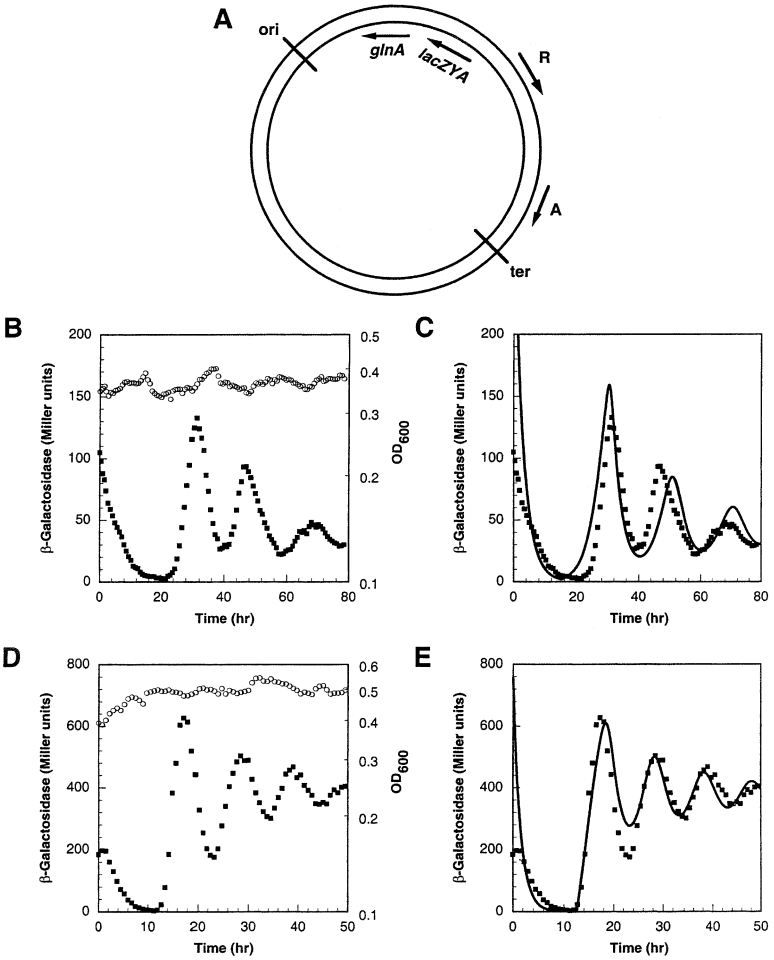

Figure 3. Three-Cycle Clock

(A) Location of the activator and repressor modules and the (natural) *lacZYA* operon. Relative positions of the repressor module (R, located in the *glnK* landing pad), activator module (A, located in the *trp* landing pad), origin of DNA replication (ori), terminus of DNA replication (ter), *glnA*, and *lacZYA* are shown.

(B) Typical clock run under conditions where cells double every 2 hr. The culture contained 0.4% w/v glucose, 0.1% w/v glutamine, 100 μg/ml ampicillin, 50 μg/ml kanamycin, and 12.5 μg/ml chloramphenicol. Solid squares, β-galactosidase activity (miller units); open circles, OD_{600}.

(C) Comparison of the data in (B) to a simulation of the experimental conditions.

(D) Typical clock run where the cells double every hour. Procedures and conditions were as in (B), except the growth medium contained in addition 0.1% w/v casein hydrolysate.

(E) Comparison of the data in (D) to a simulation of the experimental conditions.

respect to X_2 is again nearly zero. The kinetic order depends on the concentration of activator and may be zero or greater than zero. Immunoblotting analysis of the NRI level at the final steady state in a clock experiment indicated that the level of NRI was very low (data not shown). If the system is poised such that the X_2 concentration is at the low end of the regulating range, then increasing X_2 has the potential to increase the kinetic order for activation of the activator module (g_{12}) and thus to move the system into sector 4 of design space. This adjustment seeks to take better advantage of the potential cooperativity inherent in the activator module.

The simplest means of increasing the concentration of X_2 is to increase the activator module copy number. In rapidly growing *E. coli* cells, the copy number of genes located near the origin of DNA replication is about 4-fold greater than the copy number of genes located near the terminus of DNA replication. To alter the relative copy number of the activator module, we changed its position on the *E. coli* chromosome from the *trp* region near the replication terminus to the *rbs* region near the replication origin. When the configuration of modules depicted in Figure 5A were used, damped oscillations exhibiting at least 4 cycles with a 10 hr period were reproducibly obtained in experiments lasting ~50 hr (Figure 5B). We interpret these results as indicating that altering the chromosomal location of the activator module brought about a small increase in X_2 causing in an increase in g_{12}, which decreased the distance to the boundary of sector 4 thereby prolonging oscillatory behavior. Simulations with model parameters that move the clock design closer to sector 4 (Figure 1B) corresponded well to the experimental results (Figure 5C, solid lines).

Interestingly, the 4-cycle clock displayed very low levels of *lacZ* expression during the initial 10 hr of the experiments (e.g., Figures 5B and 5E, Figure 6, top). Since the initial level of β-galactosidase reflects transcription that occurred in the seed culture in the presence of IPTG, the 4-cycle clock must produce a very high level of LacI during growth in the presence of IPTG, such that *lacZYA* was repressed even though IPTG was present. This possibility was not built into our model, and thus the simulations of β-galactosidase activity do not fit well with the experimental data at the beginning of the clock experiments.

Our clock is designed to produce regular bursts of activator and repressor. In the experiments above, we measured expression of *lacZ* expression as a reporter of repressor concentration. To assess the periodicity of activator, we conducted another experiment, and assayed samples for expression of the *glnA* product, glutamine synthetase (GS, Figure 5D), the expression of *lacZ* (Figure 5E), and for the level of NRI by immunoblotting (data not shown). Combining these measurements in a

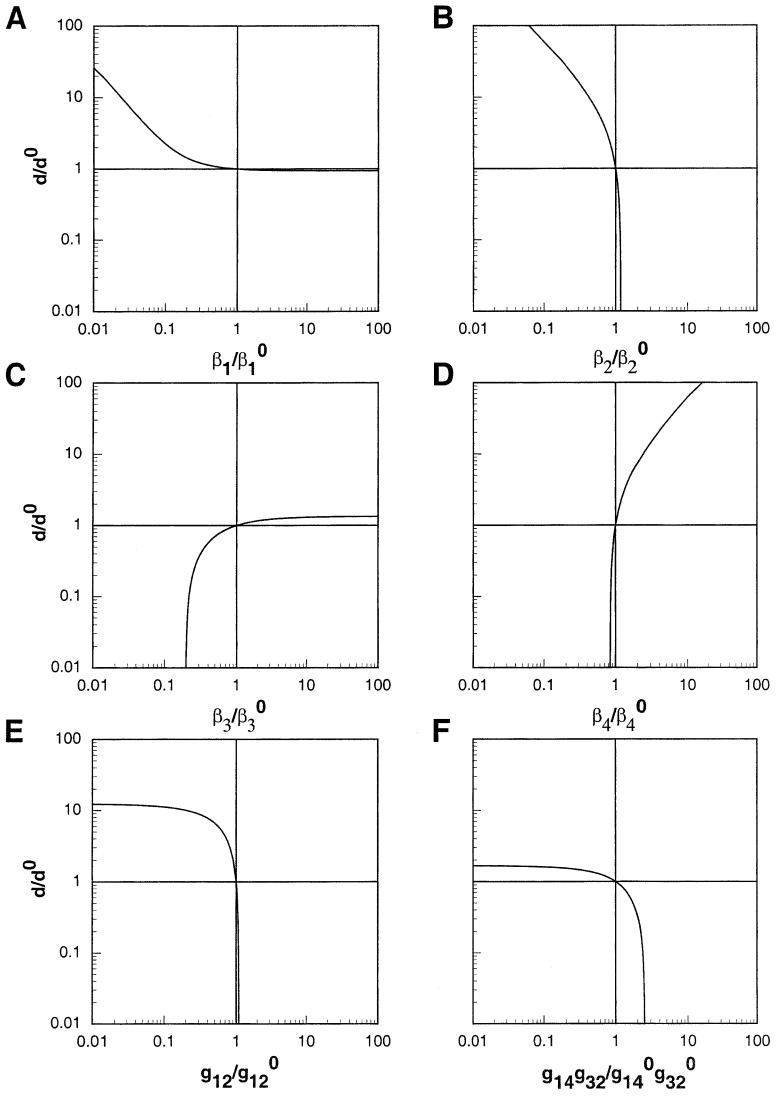

Figure 4. Sensitivity of the Distance between a Point in Sector 1 and the Boundary to Sector 4 to Alterations in Clock Parameters

(A) Sensitivity to alteration of the stability of activator module mRNA.

(B) Sensitivity to alteration of activator (NRIP) stability.

(C) Sensitivity to alteration of the stability of repressor module mRNA.

(D) Sensitivity to alteration of repressor stability.

(E) Sensitivity to alteration of the kinetic order for activation of the activator module.

(F) Sensitivity to alteration of the product of the kinetic orders for activation of the repressor module and repression of the activator module.

single experiment revealed the phasing between the clock modules, and between the NRI level and the expression of the chromosomal *glnA* gene.

Immunoblotting experiments with polyclonal anti-NRI revealed that, as anticipated, the clock results in bursts of activator synthesis that become damped over time (data not shown). A high level of NRI was only detected in samples from the early time points in the clock run; thereafter the peak NRI levels during our experiments were below the level obtained in wild-type nitrogen-starved cells, and NRI levels when the clock has reached steady state were considerably below this level (data not shown). Activation of the chromosomal *glnA* gene, as indicated by the level of GS (Figure 5D), occurred along with the bursts in activator synthesis (data not shown), with the exception that the rise in GS expression at hours 4–6 of the clock run occurred while NRI concentration was decreasing. Further investigation of this phenomenon indicated that *glnAp2* promoter expression is limited when the concentration of NRI∼P is high by the binding of NRI∼P to low-affinity sites mapping between the promoter and enhancer (Atkinson et al., 2002a). Relief from this limitation of *glnAp2* by high NRI∼P is apparently responsible for the first peak in GS activity (Figure 5D). The periodic expression of GS and β-galactosidase were slightly out of phase, as expected. Simulations with model parameters that move the clock design closer to sector 4 again corresponded well to the experimental results (Figures 5D and 5E, solid lines). Limitation of *glnAp2* by high NRI∼P was not built into the model; this probably accounts for the poor fit of the GS data at the beginning of the clock run (Figure 5D). Comparison of Figures 5C and 5E indicates the reproducibility of experiments with this clock.

Damping Is Due to Clock Design

Two hypotheses may account for the damping of oscillations displayed by our clocks. The damping may have been due to system design, that is, the system may map into sector 1 of design space (Figure 1). Alternatively, the damping may have been due to a loss of synchrony among cells that contain an undamped oscillator mapping within sector 4 of design space. For example, if the generation time of the cells within the chemostat

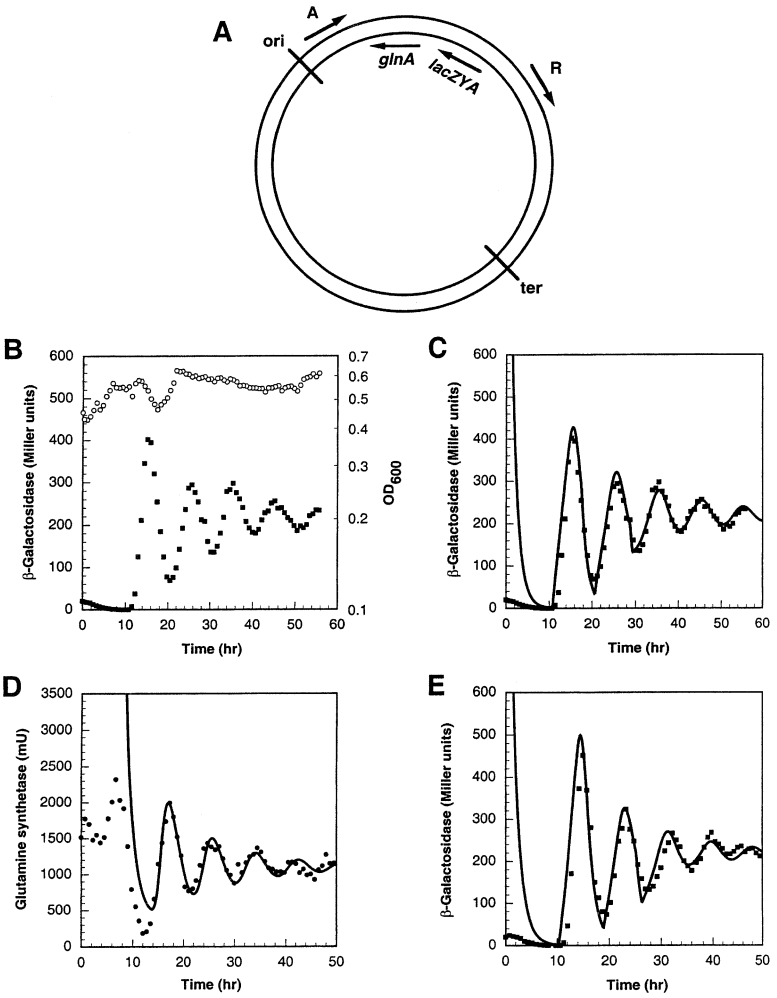

Figure 5. Four-Cycle Clock

(A) Location of activator and repressor modules, *lacZYA* operon and *glnA* gene. Symbols are as in Figure 3.

(B) Typical clock run under conditions where cells double about every hour. Media contained 1% w/v glucose, 0.1% w/v glutamine, 0.1% casamino acids, 100 μg/ml ampicillin, and 12.5 μg/ml chloramphenicol. Symbols are as in Figure 3D.

(C) Comparison of the data in (B) to the simulation of the experimental conditions.

(D) Regulation of *glnA* expression in a four-cycle clock. Experimental conditions were as in (B). Expression of *glnA* was monitored by measuring glutamine synthetase activity, expressed in mU. Comparison of data (points) to a simulation of the experimental conditions (solid line).

(E) Regulation of *lacZ* expression in the experiment depicted in (D). Comparison of data (points) to a simulation (solid line) is shown. Comparison of (C) and (E) demonstrates the reproducibility of the system.

showed significant variation, damping at the population level would be observed because perfect oscillators in individual cells would become progressively out of phase. Of course, the observed damping may be due to damped oscillators that also become out of phase. Thus, interpretation of the results required information on clock function at the single cell level. When the population achieves steady state, similar expression levels of reporter should be observed in all cells according to the former hypothesis, whereas a wide range of expression levels of reporter should be observed among cells if the latter hypothesis is true.

To examine the level of LacI at the single cell level, we used a fusion of a LacI-repressible promoter to the gene encoding cyan fluorescent protein (CFP; Elowitz et al. 2002). This reporter, in a single-copy-landing pad within the *gal* operon of *E. coli,* was introduced into the strain depicted in Figure 5A, and a standard clock experiment was performed in which 4 cycles of *lacZYA* expression were obtained (Figure 6, top). During the clock run, samples were frozen and later total fluorescence of these samples was measured and CFP expression in single cells was determined by fluorescence microscopy (Experimental Procedures). At the population level, CFP levels exhibited damped oscillations that were slightly out of phase with β-galactosidase expressed from the chromosomal *lacZ* (data not shown, see below). This is not unexpected, since the promoter driving CFP expression has a single *lac* operator, as opposed to the three operators at *lacZYA*. At the single-cell level, damping of oscillations was evident (Figure 6). Strongly fluorescent cells were only obtained at the first peak of CFP expression, and later peaks contained cells that were less fluorescent. In a separate experiment, we compared two samples with equal fluorescence, one consisting of cells from the final steady state and the other consisting of a mixture of cells from the first peak and trough. These samples were quite distinct, as only the mixture of cells from the first peak and trough had a significant fraction of highly fluorescent cells (data not shown). This suggests that the observed damping is mainly due to the clock design.

Building a Genetic Toggle Switch

Our system should produce toggle-switch behavior when parameters place it in sectors 2 or 3 of design space (Figure 1). The simplest way to reach sectors 2 or 3 is by reducing the product $g_{32}g_{14}$. The kinetic order g_{32} can be reduced to zero by disconnecting the production of repressor from activator, such as by having repressor synthesized constitutively from the natural *lacI* promoter. The resulting circuit is represented by the

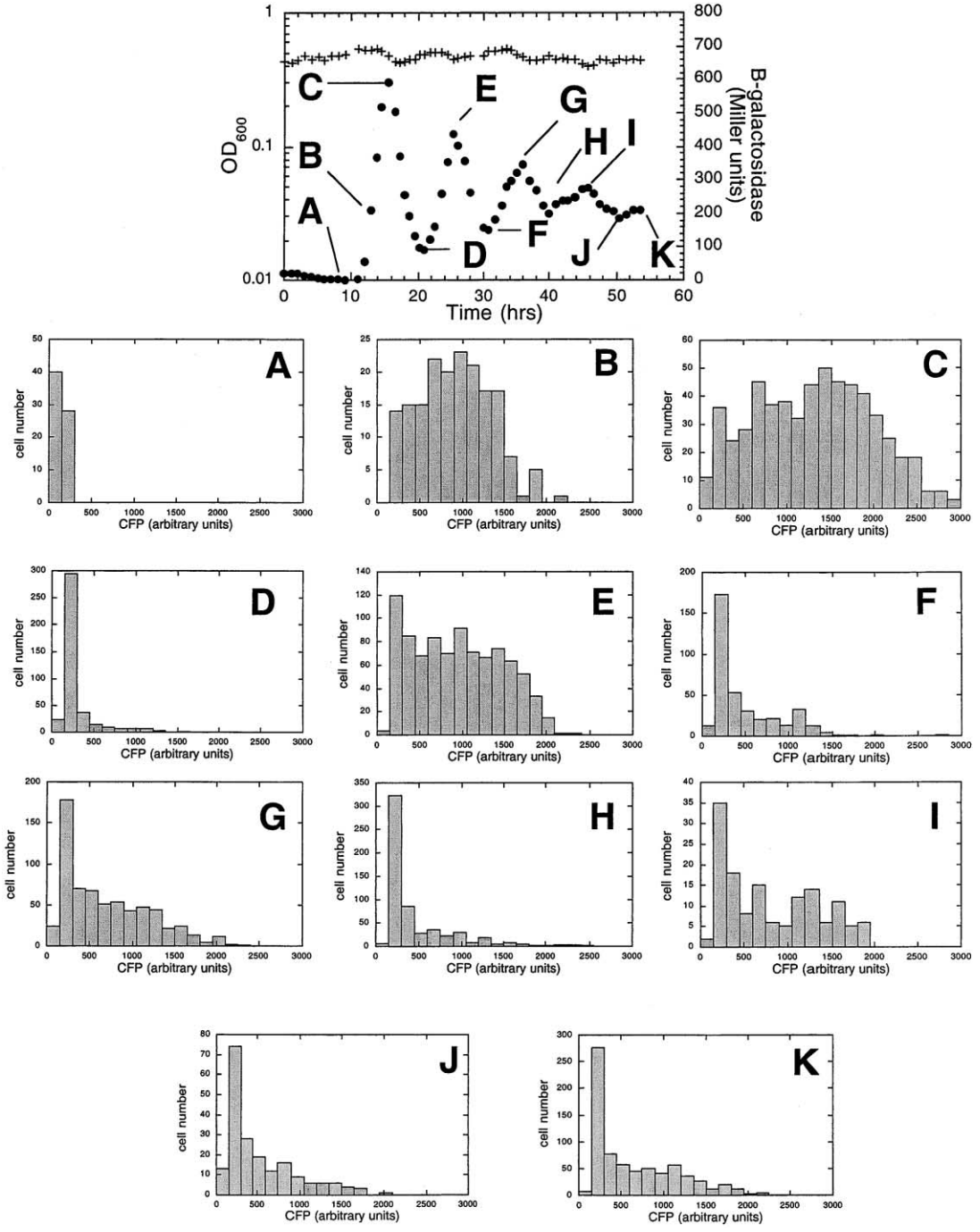

Figure 6. Expression of CFP under Control of the Genetic Clock at the Single-Cell Level

(Top) A clock run was made using cells containing CFP under the control of a LacI-repressible promoter. During the clock run, β-galactosidase expression was monitored, and samples were stored at −20°C as 40% (v/v) glycerol suspensions. Fractions analyzed are indicated by letters. (A–K) Results of fluorescent microscopy analysis (Experimental Procedures), compiled as stacked histograms in 20 bins. Different numbers of cells were analyzed for different fractions, as indicated on the vertical axis of each image.

kinetic model in Figure 1A when the vertical arrow depicting the positive influence of activator on the synthesis of X_3 is eliminated, and by the construct represented in Figure 2B. The level of effective repressor can be controlled by varying the IPTG concentration, using a *lacY* mutant strain that is unable to increase the transport of IPTG in response to induction. In this case, the only realizable models lie along the g_{12} axis in Figure 1B. If the kinetic order g_{12} is high enough, the system will fall into sector 2 (between points b and e in Figure 1B) and toggle-switch behavior should result. The prediction is then that activator concentration will switch from a low level when the system is repressed to a high level when derepressed and that the concentration of

repressor at which switching occurs will depend on the history of the system. Activator concentration was scored by measuring glutamine synthetase.

A detailed analysis of the hysteretic behavior can be found in Savageau (2002). The intuitive explanation for the hysteresis is as follows. There is a competition between activator and repressor at the promoter of the activator module. At intermediate concentrations of repressor (given indirectly by the concentration of IPTG), there is an unstable state (a balance point at which the two influences are equivalent), such that any slight positive perturbation of activator will cause the system to "run away" to the upper steady state because of the "gain" in positive feedback and any slight negative perturbation will cause the system to run away to the lower steady state because of the "loss" in positive feedback. At these intermediate concentrations of repressor (IPTG), there will be two different steady states, depending on the system history. At a sufficiently high concentration of repressor, positive feedback is effectively blocked and no positive perturbation of activator is sufficient to initiate the run away to the upper steady state. Conversely, at a sufficiently low concentration of repressor, positive feedback will dominate and no negative perturbation of activator is sufficient to initiate the run away to the lower steady state. These two concentrations of repressor (IPTG) define the two thresholds at which switching occurs on the hysteretic curve.

Cells containing the appropriate circuitry were grown overnight in the presence or absence of IPTG, washed, diluted a million-fold into media containing various concentrations of IPTG, and grown for ~17 generations, after which β-galactosidase and GS were measured. Whereas *lacZ* expression responded gradually to increasing IPTG concentration (Figure 7A), as expected, GS expression was nearly discontinuous and depended on the history of the system (Figure 7B). The basal level of *glnA* expression observed at low concentrations of IPTG reflects expression from the *glnAp1* promoter, and the increase of about 20-fold at derepressing concentrations of IPTG are due to expression from *glnAp2*. These levels of expression are consistent with previous studies of *glnA* expression (Atkinson et al., 2002a; Reitzer and Magasanik, 1985). The results indicate that the kinetic order g_{12} of this system has a value greater than 1.0 (the x-value of point b in Figure 1B) and less than the x-value of point f in Figure 1B.

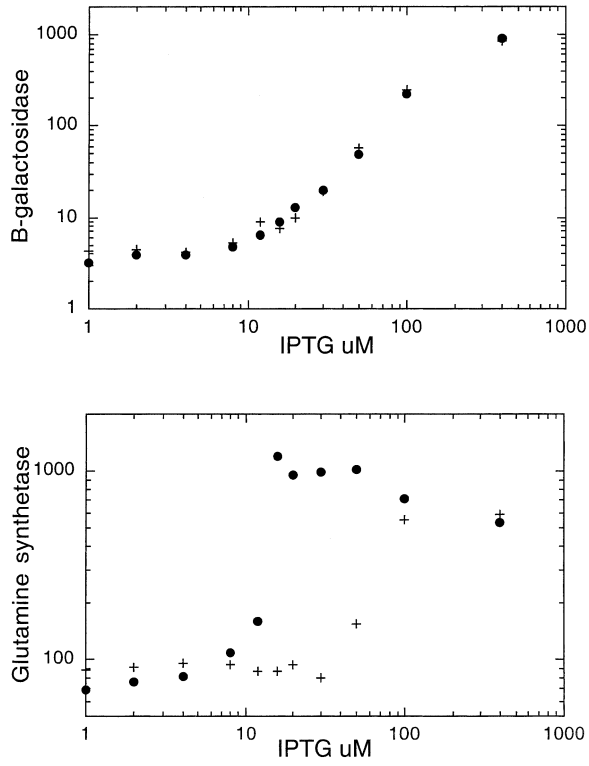

Figure 7. Toggle Switch

The strain was grown overnight in the presence of 1 mM IPTG (●) or in the absence of IPTG (+). Cells were pelleted and washed in medium-lacking IPTG, diluted a million-fold into medium containing the indicated IPTG concentration, and grown 17 generations, after which β-galactosidase (A) and glutamine synthetase (B) were measured.

Discussion

Synthetic genetic systems have the potential to advance our understanding of cellular processes. In addition to serving practical applications, these systems can facilitate the study of system design principles and advance our understanding of the natural components used as parts. Our genetic systems produce damped oscillations or toggle-switch behavior in a noise-resistant fashion in large populations of cells. The genetic stability of these systems, the availability of a model that approximates their behavior, and the modular nature of their design render them useful tools for further study.

The circuits are comprised of activator and repressor modules. The activator module for both the clock and the toggle switch contains a modified form of the *glnA* promoter driving expression of the activator NRI. The *glnA* promoter was modified to include operator sites for the LacI repressor in addition to the normal enhancer sites for NRI~P, thereby connecting the output of the repressor module to the input of the activator module. The repressor module for the clock consists of the *glnK* promoter, which also is activated by NRI~P, fused to the structural gene *lacI*. This design connects the output of the activator module to the input of the repressor module. The repressor module for the toggle switch is the native transcriptional unit for the LacI repressor, which is constitutive and disconnected from the output of the activator module.

Our clock was developed without a complete set of biochemical parameters for the interactions that it employs. Our method was designed to circumvent this absence of biochemical information, and thus may be applicable to other genetic engineering projects. Initially, we explored the capabilities of models in general terms, where the relationship among parameters was considered as opposed to the values of the parameters themselves. Models not feasible to build or test were rejected without detailed analysis. Models were then explored to determine whether there is a region of realizable design space showing the desired behavior. In our case, we saw that realizable designs derived from the model in

Figure 1A could produce toggle switch behavior, damped oscillations, or stable oscillations.

Owing to our incomplete knowledge of the biological components, it is not possible to perfectly realize the model in cells. Nevertheless, practical steps can be taken. Well-studied components were used, and, to increase genetic stability of the system, the clock modules were maintained on the chromosome at unique locations, as they are in the natural clocks. The initial goal was to determine the general pattern of reporter expression, that is, to see within which sector of design space the initial design maps. The strain depicted in Figure 3 reproducibly exhibited damped oscillations with three unambiguous cycles. Thus, this design mapped to sector 1 in Figure 1B.

We analyzed the model to identify the parameters that have the greatest effect on moving the design into the desired sector of design space where stable oscillations are produced. The best strategy for generating sustained oscillations would be to decrease the life time of activator protein, increase the life time of repressor mRNA, and increase the cooperativity of the regulatory interactions (g_{12}, g_{32}, and g_{14}). Of these, the easiest to alter is g_{12}, which is predicted to depend on activator concentration. Moving the activator module to a location near the origin of DNA replication, which modestly increased its copy number, reduced damping. We can quantify damping by estimating the exponential decay for the envelope of the oscillations (as if the clocks were simply linear systems), and express damping as the ratio of the half-life to the period. Using the data from experiments with similar growth conditions, for our three-cycle clock (Figure 3D) this ratio was 0.94; for our four-cycle clock ratios of 1.2 (Figure 5B), 1.3 (Figure 5E), and 1.1 (Figure 6, top) were obtained. This ~20% decrease in damping resulted in an additional cycle. Clearly, chromosomal location influenced the activity of the activator module in *E. coli*.

Further studies of the clock will consist of efforts to increase the resemblance of the prototype to the model, such as by eliminating the low affinity NRI binding sites within the activator module and eliminating other cellular binding sites for activator and repressor, and by conducting a systematic search of parameter space. The modular design of our system renders essentially all parameters accessible to experimental manipulation. Thus, the model may be quickly evaluated and refined simply by observing of the effects of parameter manipulation on system performance, without detailed biochemical information on the underlying regulatory interactions. All one needs is qualitative information that the desired parameter has indeed been altered in the desired direction and that the other parameters of the system have not been altered in the process. By an iterative process of modeling and experiment, synthetic genetic systems with desired characteristics may then be produced.

Experimental Procedures

Modeling

The dynamic behavior of the model in Figure 1A is determined by the first 4 stages of the cascade (the remaining 2 stages represent the read-out mechanism that simply tracks the level of LacI). The kinetic structure of this model is essentially the same as a previously analyzed model for the gene circuit of a repressible biosynthetic system with an autogenously regulated activator (Savageau, 1975, 1976). In the earlier studies, the focus was on the conditions for the nominal steady state to be locally stable, whereas here we were concerned with the conditions for the nominal steady state to be locally unstable, a necessary condition for sustained oscillations.

Modeling of the dynamic behavior of the systems and analysis of the geometry of design space are presented in detail in the Supplemental Data available at http://www.cell.com/cgi/content/full/113/5/597/DC1.

Strains and Plasmids

Detailed descriptions of the strains and plasmids used in this work and their construction are provided in the Supplemental Data available at http://www.cell.com/cgi/content/full/113/5/597/DC1. The relevant genotype of the bacterial strains used for the experiments in the Figures is as follows: Figure 3: *lacI*$^-$ *ΔglnLG trp::ϕ(glnAp-lacOperfect-glnG)..kan*^{r} *Δmdl-glnK::ϕ(glnKp-lacI) amtB::cam*^{r}*/p3Y15 amp*^{r} *glnL2302*; Figure 5: *lacI*$^-$ *ΔglnLG ΔrbsDACBK::ϕ(glnAp-lacOperfect-glnG)..gent*^{r}*Δmdl-glnK::ϕ(glnKp-lacI) amtB::cam*^{r}*/p3Y15 amp*^{r} *glnL2302*; Figure 6: *lacI*$^-$ *ΔglnLG ΔrbsDACBK::ϕ(glnAp-lacOperfect-glnG)..gent*^{r} *Δmdl-glnK::ϕ(glnKp-lacI) amtB::cam*^{r} *gal: ϕ(pO+-cfp)..amp*^{r}/p3Y15K *kan*^{r} *glnL2302*; Figure 7: *lacI*$^+$, *lacZ*$^+$*Y*$^-$*A*$^+$ *ΔglnLG, ΔrbsDACBK::ϕ(glnAp-lacOperfect-glnG)..gent*^{r}*/p3Y15 amp*^{r} *glnL2302*.

Growth Conditions

The growth medium contained W-salts (Rothstein et al., 1980), supplemented with 0.004% w/v thiamine and 0.004% w/v tryptophan. Carbon and nitrogen sources and antibiotics are indicated in the figure legends. For clock experiments, overnight cultures were grown in the indicated medium + 0.1 mM IPTG at 30°C for 19–22 hr. The cells were then washed and used to inoculate a 1L chemostat (New Brunswick Scientific) containing medium lacking IPTG. Culture volume was ~375 ml (~10^{11} cells). Turbidity was held constant by manual adjustment of the nutrient pump. The culture was vigorously aerated and stirred; incubation was at 25°C. Samples were obtained from the efflux tube of the chemostat.

For toggle-switch experiments, the strain was grown overnight at 37°C in medium containing ampicillin (100 μg/mL), with glucose (0.4% w/v) as carbon source and glutamine (0.2% w/v) and casein hydrolysate (0.1% w/v) as nitrogen sources, and either containing or lacking 1 mM IPTG. Cells were pelleted and washed in medium-lacking IPTG, diluted a million-fold into fresh medium containing the indicated concentration of IPTG, and grown for ~17 generations at 37°C, after which β-galactosidase and glutamine synthetase were measured.

β-Galactosidase and Glutamine Synthetase Assay

β-galactosidase, expressed in miller units, was assayed immediately after sampling using 0.1% SDS and chloroform-permeablized cells (Silhavy et al., 1984). The γ-glutamyl transferase activity of GS (nmol glutamyl-hydroximate formed/min/mg protein) was assayed as described (Rhee et al., 1985). Protein determinations were by the method of Lowry et al. (1951).

Western Blotting

Crude protein extracts were resolved on 10% SDS-PAGE acrylamide gels, transferred to nitrocellulose, and probed using anti-NRI generously provided by L.J. Reitzer. Development employed the Amersham-Pharmacia ECL detection system.

Fluorescence Microscopy

Samples from a clock run (Figure 6, top) were collected and stored as a suspension of cells in 40% glycerol at −20°C. For measurement of total fluorescence, 1 ml of each stored sample was examined using a SLM Aminco SPF-500 fluorimeter. For fluorescence microscopy, cells were pelleted and resuspended in 1/10 volume Tris-buffered saline, and 5 μl of the concentrated cell suspension was applied to polylysine-coated slides. Phase and fluorescent images were obtained using a Nikon TE-300 inverted microscope at 600× magnification. Images were collected and processed using Metamorph software (Universal Imaging, West Chester, PA). Regions of

the phase images corresponding to cells were obtained by specifying threshold levels manually. A binary mask was then applied to the corresponding CFP image. Well-focused and well-isolated cells in the phase images were selected, and the average pixel intensity in the corresponding regions from the CFP image was recorded. All of our measurements were below the maximum value detectable in this system (4096 arbitrary units). Background fluorescence of nonfluorescent cells was about 50 arbitrary units, using this system.

To compare the final steady-state culture to a mixture of cells from the first peak and trough, cells from the −20°C samples corresponding to the first peak of fluorescence (fraction 16, the fraction immediately preceding the fraction marked "C" in Figure 6) and first trough of fluorescence (fraction 23, marked "D" in Figure 6) were examined separately, as was fraction 58 (marked "K" in Figure 6), corresponding to the final steady state. For comparison, a mixture of fraction 16 and fraction 23 having fluorescence equal to fraction 58 was examined.

Acknowledgments

Supported by grant R01-GM63642. We thank M. Elowitz for providing strain RP22; L.J. Reitzer for providing polyclonal anti-NRI; T.A. Blauwkamp for assistance and suggestions during the early stages of the project; and B. Magasanik, T.J. Silhavy, and J.V. Ninfa for useful discussions. We thank J. Swanson for helpful discussions and for guiding our single-cell studies, which were performed in his laboratory, and A. Hoppe for advice and technical assistance.

Received: June 24, 2002
Revised: March 28, 2003
Accepted: April 10, 2003
Published: May 29, 2003

References

Atkinson, M.R., Pattaramanon, N., and Ninfa, A.J. (2002a). Governor of the *glnAp2* promoter of *Escherichia coli*. Mol. Microbiol. *46*, 1247–1257.

Atkinson, M.R., Blauwkamp, T.A., Bondarenko, V., Studitsky, V., and Ninfa, A.J. (2002b). Activation of the *glnA*, *glnK*, and *nac* promoters as *Escherichia coli* undergoes the transition from nitrogen excess growth to nitrogen starvation. J. Bacteriol. *184*, 5358–5363.

Barkai, N., and Leibler, S. (2000). Biological rhythms: circadian clocks limited by noise. Nature *403*, 267–268.

Beckwith, J. (1987). In *Escherichia coli* and *Salmonella typhimurimum*, Cellular and Molecular Biology, F.C. Neidhardt, J.L. Ingraham, K.B. Low, B. Magasanik, M. Schaechter, H.E. Umbarger, eds. (Washington D.C.: ASM Press), pp. 1444–1452.

Blauwkamp, T.A., and Ninfa, A.J. (2002). Physiological role of the GlnK signal transduction protein of *Escherichia coli*: survival of nitrogen starvation. Mol. Microbiol. *46*, 203–214.

Chen, Y.-M., Backman, K., and Magasanik, B. (1982). Characterization of a gene, *glnL*, the product of which is involved in the regulation of nitrogen utilization in *Escherichia coli*. J. Bacteriol. *150*, 214–220.

Elliot, T. (1992). A method for constructing single-copy *lac* fusions in *Salmonella typhimurium* and its application to the *hemA-pfrA* operon. J. Bacteriol. *174*, 245–253.

Elowitz, M.B., and Leibler, S. (2000). A synthetic oscillatory network of transcriptional regulators. Nature *403*, 335–338.

Elowitz, M.B., Levine, A.J., Sigga, E.D., and Swain, P.S. (2002). Stochastic gene expression in a single cell. Science *297*, 1183–1186.

Gardner, T.S., Cantor, C.R., and Collins, J.J. (2000). Construction of a genetic toggle switch in *Escherichia coli*. Nature *403*, 339–342.

Kondo, T., Mori, T., Lebedeva, N.V., Aoki, S., Ishiura, M., and Golden, S. (1997). Circadian rhythms in rapidly dividing cyanobacteria. Science *275*, 224–227.

Lowry, O.H., Rosebrough, N.J., Farr, A.L., and Randall, R.J. (1951). Protein measurement with the folin phenol reagent. J. Biol. Chem. *193*, 265–275.

Mori, T., Binder, B., and Johnson, C.H. (1996). Circadian gating of cell division in cyanobacteria growing with average doubling times of less than 24 hours. Proc. Natl. Acad. Sci. USA *93*, 10183–10188.

Ninfa, A.J., and Magasanik, B. (1986). Covalent modification of the *glnG* product, NRI, by the *glnL* product, NRII, regulates the transcription of the *glnALG* operon in *Escherichia coli*. Proc. Natl. Acad. Sci. USA *83*, 5909–5913.

Ninfa, A.J., Reitzer, L.J., and Magasanik, B. (1987). Initiation of transcription at the bacterial *glnAp2* promoter by purified *E. coli* components is facilitated by enhancers. Cell *50*, 1039–1046.

Ninfa, A.J., Jiang, P., Atkinson, M.R., and Peliska, J.A. (2000). Integration of antagonistic signals in the regulation of nitrogen assimilation in *Escherichia coli*. Curr. Top. Cell. Regul. *36*, 31–75.

Oehler, S., Eismann, E.R., Kramer, H., and Muller-Hill, B. (1990). The three operators of the *lac* operon cooperate in repression. EMBO J. *9*, 973–979.

Reitzer, L.J., and Magasanik, B. (1985). Expression of *glnA* in *Escherichia coli* is regulated at tandem promoters. Proc. Natl. Acad. Sci. USA *82*, 1979–1983.

Rhee, S.G., Chock, P.B., and Stadtman, E.R. (1985). Glutamine synthetase from *Escherichia coli*. Methods Enzymol. *113*, 213–241.

Rothstein, D.M., Pahel, G., Tyler, B., and Magasanik, B. (1980). Regulation of expression from the *glnA* promoter of *Escherichia coli* in the absence of glutamine synthetase. Proc. Natl. Acad. Sci. USA *77*, 7372–7376.

Savageau, M.A. (1975). Significance of autogenously regulated and constitutive synthesis of regulatory proteins in repressible biosynthetic systems. Nature *258*, 208–214.

Savageau, M.A. (1976). Biochemical Systems Analysis: A Study of Function and Design in Molecular Biology (Reading, MA: Addison-Wesley).

Savageau, M.A. (2002). Alternative designs for a genetic switch: Analysis of switching times using the piece-wise power-law representation. Math. Biosci. *180*, 237–253.

Silhavy, T.J., Berman, M.L., and Enquist, L.W. (1984). Experiments with Gene Fusions (Cold Spring Harbor, N.Y.: Cold Spring Harbor Laboratory), pp. 107–111.

Simons, R.W., Houman, F., and Kleckner, N. (1987). Improved single copy and multicopy *lac*-based cloning vectors for protein and operon fusions. Gene *53*, 85–96.

Su, W., Porter, S., Kustu, S., and Echols, H. (1990). DNA-looping and enhancer activity: association between DNA-bound NtrC activator and RNA polymerase at the bacterial *glnA* promoter. Proc. Natl. Acad. Sci. USA *87*, 5504–5508.